Journal of Tissue Engineering
Volume 9: 1–10

DOI: 10.1177/2041731418807396
journals.sagepub.com/home/tej
SAGE

Reformulated mineral trioxide aggregate components and the assessments for use as future dental regenerative cements

Ho-Jin Moon[1,2], Jung-Hwan Lee[2,3,4], Joong-Hyun Kim[2,5], Jonathan C Knowles[4,6,7,8], Yong-Bum Cho[1], Dong-Hoon Shin[1], Hae-Hyoung Lee[2,3,4] and Hae-Won Kim[2,3,4,8]

Abstract

Mineral trioxide aggregate, which comprises three major inorganic components, namely, tricalcium silicate (C3S), dicalcium silicate (C2S), and tricalcium aluminate (C3A), is promising regenerative cement for dentistry. While mineral trioxide aggregate has been successfully applied in retrograde filling, the exact role of each component in the mineral trioxide aggregate system is largely unexplored. In this study, we individually synthesized the three components, namely, C3S, C2A, and C3A, and then mixed them to achieve various compositions (a total of 14 compositions including those similar to mineral trioxide aggregate). All powders were fabricated to obtain high purity. The setting reaction of all cement compositions was within 40 min, which is shorter than for commercial mineral trioxide aggregate (~150 min). Over time, the pH of the composed cements initially showed an abrupt increase and then plateaued (pH 10–12), which is a typical behavior of mineral trioxide aggregate. The compression and tensile strength of the composed cements increased (2–4 times the initial values) with time for up to 21 days in an aqueous medium, the degree to which largely depended on the composition. The cell viability test with rat mesenchymal stem cells revealed no toxicity for any composition except C3A, which contained aluminum. To confirm the in vivo biological response, cement was retro-filled into an extracted rat tooth and the complex was re-implanted. Four weeks post-operation, histological assessments revealed that C3A caused significant tissue toxicity, while good tissue compatibility was observed with the other compositions. Taken together, these results reveal that of the three major constituents of mineral trioxide aggregate, C3A generated significant toxicity in vitro and in vivo, although it accelerated setting time. This study highlights the need for careful consideration with regard to the composition of mineral trioxide aggregate, and if possible (when other properties are satisfactory), the C3A component should be avoided, which can be achieved by the mixture of individual components.

Keywords

Mineral trioxide aggregate, tricalcium silicate, dicalcium silicate, tricalcium aluminate, intentional replantation

Date received: 30 July 2018; accepted: 26 September 2018

[1]Department of Conservative Dentistry, College of Dentistry, Dankook University, Cheonan, Republic of Korea
[2]Institute of Tissue Regeneration Engineering (ITREN), Dankook University, Cheonan, Republic of Korea
[3]Department of Biomaterials Science, College of Dentistry, Dankook University, Cheonan, Republic of Korea
[4]UCL Eastman-Korea Dental Medicine Innovation Centre, Dankook University, Cheonan, Republic of Korea
[5]Laboratory Animal Center, Osong Medical Innovation Foundation, Cheongju, Republic of Korea
[6]Division of Biomaterials and Tissue Engineering, Eastman Dental Institute, University College London, London, UK
[7]The Discoveries Centre for Regenerative and Precision Medicine, Eastman Dental Institute, University College London, London, UK
[8]Department of Nanobiomedical Science and BK21 PLUS NBM Global Research Center for Regenerative Medicine, Dankook University, Cheonan, Republic of Korea

Corresponding author:
Hae-Won Kim, Institute of Tissue Regeneration Engineering (ITREN), Dankook University, Cheonan 31116, Republic of Korea.
Email: kimhw@dku.edu

Introduction

Mineral trioxide aggregate (MTA), developed by Dr Mahmoud Torabinejad based on Portland cement three decades ago, comprises fine hydrophilic powders containing calcium, silicon, and bismuth oxide, which are set in the presence of water.[1,2] MTA, a calcium silicate-based cement, has been widely used in dental clinics for root canal retro-filling, base, pulp capping, and perforation repair due to its outstanding dental tissue regenerative potential, bioactivity, sealing ability, and biocompatibility.[2–5] Since MTA is basically fabricated from Portland cement after excluding the toxic metal complex, the MTA has three essential components and a single modifier, namely, tricalcium silicate (C3S), dicalcium silicate (C2S), tricalcium aluminate (C3A), and bismuth oxide for radiopacity.[6]

From the beginning, the retro-filling of MTA has been carried out to regenerate apical hard tissue with intentional tooth extraction or apicoectomy and considered as a standard clinical procedure in case of occurrence of apical lesion around root after root canal therapy.[7] With its widespread use, the biocompatibility of MTA has been investigated to find the safety in clinical settings. Generally, in vitro studies show that the MTA is biocompatible.[8] Furthermore, there was no difference in cytotoxicity between Portland cement and MTA due to their similar compositions, with the exception of bismuth oxide (20%–25%).[9] Trace elements such as arsenic, chromium, and lead were lower in MTA than in Portland cement, so MTA revealed better proliferative and regenerative capacity.[10] A number of biocompatibility and mutagenicity studies have shown that MTA is a biocompatible material.[7] In fact, the results of a meta-analysis on MTA biocompatibility showed that MTA is more biocompatible than traditional retro-filling materials such as Super EBA®, IRM®, and silver amalgam.[11] However, clinical failure has been reported, which was not due to malpractice by clinicians but from other possible causes, such as insufficient regenerative potential, a lack of anti-bacterial effects, discoloration, and toxic elute from set MTA.[12–15] Heavy metal elements such as magnesium, iron, arsenic, chromium, and lead have been raised as a cause of toxicity, and many efforts have been devoted to exclude such unessential elements.[16] However, to the best of our knowledge, the adverse effects of C3A, one of the major components of MTA, that is possibly ascribed to the release of aluminum ions, have not been investigated in detail.

Therefore, the purpose of this investigation was to determine whether C3A, one of the major fractions of MTA (~10%), adversely affected biocompatibility in vitro and in vivo, as well as any other properties of MTA. It was expected that the results of this study would show that the possibility of excluding C3A from MTA would result in better biocompatibility. To test the above hypothesis, the three major components of MTA (C3S, C2S, and C3A) were individually fabricated per the sol–gel method, and cements from the single composition or their combinations close to the ratio of compositions in MTA (total 14 compositions) were compared with MTA in terms of physical, mechanical, and biological performance.

Materials and methods

Synthesis of calcium powder

C3S, C2S, and C3A were individually fabricated by serial procedures: sol–gel process and continuous heat treatments according to previous literature.[17] For fabrication of the C3S powder, 0.3 M of calcium nitrate tetrahydrate was stirred in the solution, consisting of 70% ethanol, 5% polyethylene glycol (Mw 10,000), 1% 1 M HCl, and 0.1 M of tetraethyl orthosilicate (TEOS), at 60°C for 3 h. The mixed solution was maintained at 70°C until gelation occurred and dried at 120°C for 1 day. After calcination at 500°C for 1 h and at 1200°C for 3 h, the resultant was pulverized and heat treated at 1450°C for 8 h and for 10 h, respectively. The obtained powder was pulverized and then sieved using a 45-μm sieve. In the case of the C2S powder, 0.2 M of calcium nitrate tetrahydrate was added to the above solution and a process similar to that described above was performed except for heat treatment at 1000°C. For the C3A powder, 0.2 M of aluminum nitrate nonhydrate and 0.3 M of calcium nitrate tetrahydrate were added in distilled water (DW) with 5 wt% polyvinyl alcohol (PVA) and mixed for 5 h. The gel was obtained by holding at 60°C for 2 days, and it was then dried at 120°C for 24 h. After grinding, it was heat treated at 500°C for 1 h, then pulverized again and heat treated at 1350°C. The obtained powder was pulverized and then sieved using a 45-μm sieve.

Powder analysis

The crystal structure of the three synthesized materials was determined by X-ray diffraction (XRD; Ultima IV, Rigaku, Japan). The specimens were scanned with a range of diffraction angle of $2\theta = 10°–80°$, with a rate of 2° min^{-1} and step width of 0.02°, using Cu Kα1 radiation at 2 kV and 40 mA. ProRoot® MTA and bismuth oxide were also characterized as controls. The surface morphology of each powder was observed by a scanning electron microscope (SEM; JEOL-JSM 6510, Tokyo, Japan) at an accelerating voltage of 10 kV. The powder size distribution was determined using a particle size analyzer (Malvern Mastersizer MS2000; Malvern Instruments, Malvern, UK). Suspensions were prepared with 50 mL of ethanol and 50 μg of C3S, C2S, C3A, and ProRoot MTA. The D50 (a cumulative 50% point of diameter) of MTA, C3S, C2S, and C3A was determined as the representative size of the powder.

Physical properties

The setting time of the cement was performed with ISO 6876.[18] Briefly, a Teflon mold with a diameter of 10 mm and a height of 2 mm was used according to ISO 6876. The liquid (DW)/powder (L/P) ratio was 0.3, and it was stored in a constant temperature water bath at 100% humidity and 37°C within 2 min after mixing. The initial setting time was measured by a Gilmore needle (100 g, ϕ = 2 mm) with an interval of 30 s (n = 3). The duration of time from mixing to the point when the needle does not mark the surface with a complete circular indentation was calculated as the initial setting time. To measure the change in pH after mixing, specimens mixed with an L/P ratio of 0.3 were prepared with a diameter of 6 mm and a height of 2 mm and cured at a temperature of 37°C and a humidity of 100% for 3 h. Each specimen was placed in 10 mL of DW and 10 mL of phosphate-buffered saline (PBS). The pH was obtained by a pH meter (n = 3, Orion 3 Star; Thermo Scientific, Singapore) at 0, 20, 30, 60, 120, 240, 480, 1440, 2880, and 5760 min.

Mechanical properties

For the compressive strength test, cylinder-type specimens with a diameter of 4 mm and a height of 6 mm were prepared by mixing for 2 min at an L/P ratio of 0.3 according to the ISO 9917-1. For the diametral tensile strength test, disk specimens with a diameter of 6 mm and a height of 4 mm were prepared and the test was performed according to the protocol elsewhere.[19] The specimens were then stored in simulated body fluid (SBF) at 37°C and 100% relative humidity for 1, 7, 14, and 28 day(s) according to previous protocols.[19] Compressive and diametral tensile strength were measured using a universal testing machine (Instron 3344; Instron Corp, Canton, MA, USA) at a crosshead speed of 0.5 mm/min (n = 5).

Cytocompatibility

Rat mesenchymal stem cells (rMSCs) were collected from the femur and tibia bone marrow of 5-week-old male rats according to a previous protocol.[20] The rMSCs were cultured in three passages. A total of 1000 cells were seeded in 96-well plates and cultured for 24 h for cell attachment. The eluted solution (50% and 100%) from each disk specimen (ϕ = 10 mm and h = 2 mm) was placed in 10 mL of supplemented culture media (Dulbecco's Modified Eagle Medium (DMEM) containing 10% fetal bovine serum (FBS) and 1% Pen-Strep), then applied to each well and incubated at 37°C for 3 days. Each disk was made from Teflon mould (ϕ = 10 mm and h = 2 mm) and incubated for 3 h at 37°C at 100% humidity before extraction. Cells cultured in the culture medium without the eluent were used as a control group. Cell proliferation was measured using a cell counting kit-8 (CCK-8) as instructed by the manufacturer (Dojindo Molecular Technologies, Inc.). At the end of each culture time, 10 μL of CCK-8 solution was added to each well of 96-well plates, and the plates were incubated for 2 h at 37°C. The absorbance of each specimen was measured at a wavelength of 450 nm using a microplate (n = 4, iMark; BioRad, Hercules, CA, USA). The results were normalized to the value of the culture medium in the control group.

In vivo implantation

The experimental protocol was approved by the Institutional Animal Care and Use Committee (IACUC) of Dankook University, Republic of Korea (approval DKU-13-031). A total of 36 male, 11-week-old Sprague-Dawley rats weighing 350–400 g were used. Each rat was injected intramuscularly to the right quadriceps muscle using 80 mg/kg Zoletil and 10 mg/kg xylazine. Lidocaine (0.5%) was injected topically into the gingiva of the maxilla premaxilla. The rats were placed in the dorsal recumbent position and the surgical site was disinfected with 10% povidone iodine and 70% ethyl alcohol for an aseptic procedure. All instruments were sterilized before surgery and all procedures (n = 4) were performed aseptically according to previous intentional implantation methodology.[21] Sample size was based on previous literatures to screen the biocompatibility of different reformulated MTA compositions at apical lesion.[22–24] The rats were housed in a room at 20°C–24°C and 30%–70% relative humidity, with a 12-h daytime and 12-h night-time cycle. Rats were fed a standardized diet consisting of crushed pellet food and water. The rats were sacrificed at 4 weeks after surgery for sampling of the surrounding tissue. The specimens were harvested from each animal on postoperative week 4 and the samples were fixed in 10% neutral buffered formaldehyde solution for at least 24–48 h. The samples were reconstructed using an in vivo microcomputed tomography (μCT) system (Skyscan 1176; Skyscan, Aartselaar, Belgium) and the NRecon μCT Skyscan reconstruction software to evaluate tissue recovery. Non-decalcified cut and ground sections of the specimens in situ were prepared with the Exakt technique (Exakt Apparatebau, Norderstedt, Germany). The resin block specimens were cut into two halves along the long axis of the incisor. The initially cut sections of 200 μm were ground down to approximately 25 μm. Histology of haematoxylin and eosin (H&E) stained tissue was evaluated with a light microscope (IX71; Olympus, Tokyo, Japan) and MetaMorph® software (Molecular Devices, San Jose, CA, USA).

Statistics

Statistical analysis was performed with a one-way analysis of variance (ANOVA) with Tukey's honest significant

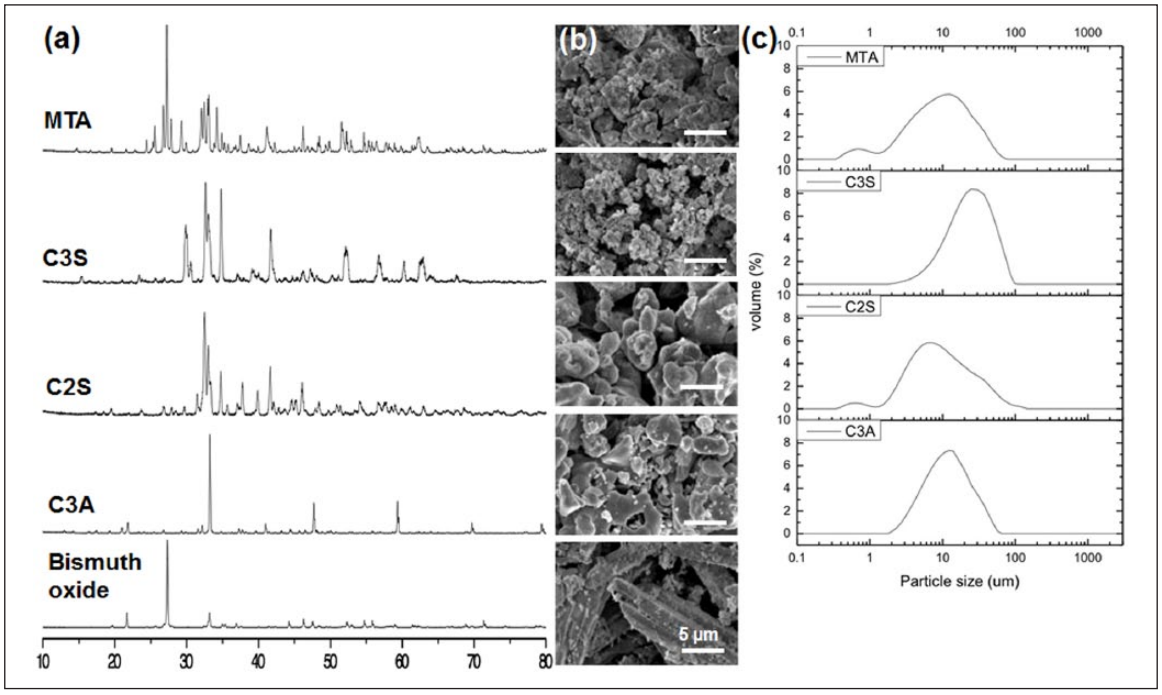

Figure 1. Characterization of the powder. After individual synthesis of the three major components of MTA (C3S, C2S, and C3A), (a) XRD, (b) SEM, and (c) laser diffraction analysis were performed to investigate the crystal structure, morphology, and size distribution of MTA, C3S, C2S, and C3A. Successful fabrication of the three powders (C3S, C2S, and C3A) with comparable size and shape was performed. All scale bars from SEM are 5 μm.

differences test as a post hoc test (IBM SPSS Statistics v23.0; IBM Corp., Armonk, NY, USA) ($p = 0.05$). Normal distribution test was performed by Shapiro–Wilk test.

Results and discussion

Synthesis of individual powder and characterization

The crystal structure of the three synthesized materials was determined by XRD. Figure 1(a) shows the typical XRD peaks of each powder (C3S, C2S, and C3A) and bismuth oxide, matched with the JCPDS (Joint Committee on Powder Diffraction Standards) card of each powder. In line with the previous literature, MTA appeared to have peaks of the combination from C3S, C2S, C3A, and bismuth oxide.[25] Subsequently, the morphology and size distribution of the powder were analyzed by SEM and laser diffraction. The SEM results revealed an irregularly shaped powder of up to ~20 μm in all groups (Figure 1(b)) except bismuth. The average sizes (D50, a cumulative 50% point of diameter) of each powder (MTA, C3S, C2S, and C3A), measured by dynamic laser scattering, were determined to be 9.0, 22.6, 8.4, and 12.0 μm, respectively (Figure 1(c)), which being considered reasonable when ground and sieved through a 45-μm pore.

Characterization of cements

After the three powders were synthesized to MTA powder, the components of C3S, C2S, and C3A were set to have a close compositional ratio to that of MTA. C3S, C2S, C3A, and MTA were also included in the experimental group as controls. The compositional information from all 14 groups is provided in the ternary graph in Figure 2(a). The L/P ratio was set at 0.3, and a Gilmore needle was utilized for measuring the initial setting time according to the ISO standard for MTA. The initial time was the longest in the MTA group (150 ± 5 min)[26] and the shortest in group 13 (Figure 2(b); C3A only, 1 ± 0.2 min). Liu et al.[27] and Liu and Chang[28] also reported that the addition of C3A quickly set C3S and C2S. The difference in setting time between this investigation and other studies may be due to powder size, phage, and the L/P ratio.[29] A decrease in setting time seemed to occur with an increase in the amount of C3A in the groups consisting of the three powder mixtures (0% C3A (1, 2, 3) > 10% C3A (4, 5, 6, 7) > 20% C3A (8,9,10)), which is due to the fast cementation between aluminum ions and calcium silica powder and is consistent with other reports.[30]

After 3 h of mixing, the specimens were put in DW (pH 5.9) or PBS (pH 7.3) for up to 4 days in order to measure the change in pH. In DW, the change in pH was similar in all groups, with a burst increase to a pH 9–10 within 20 min

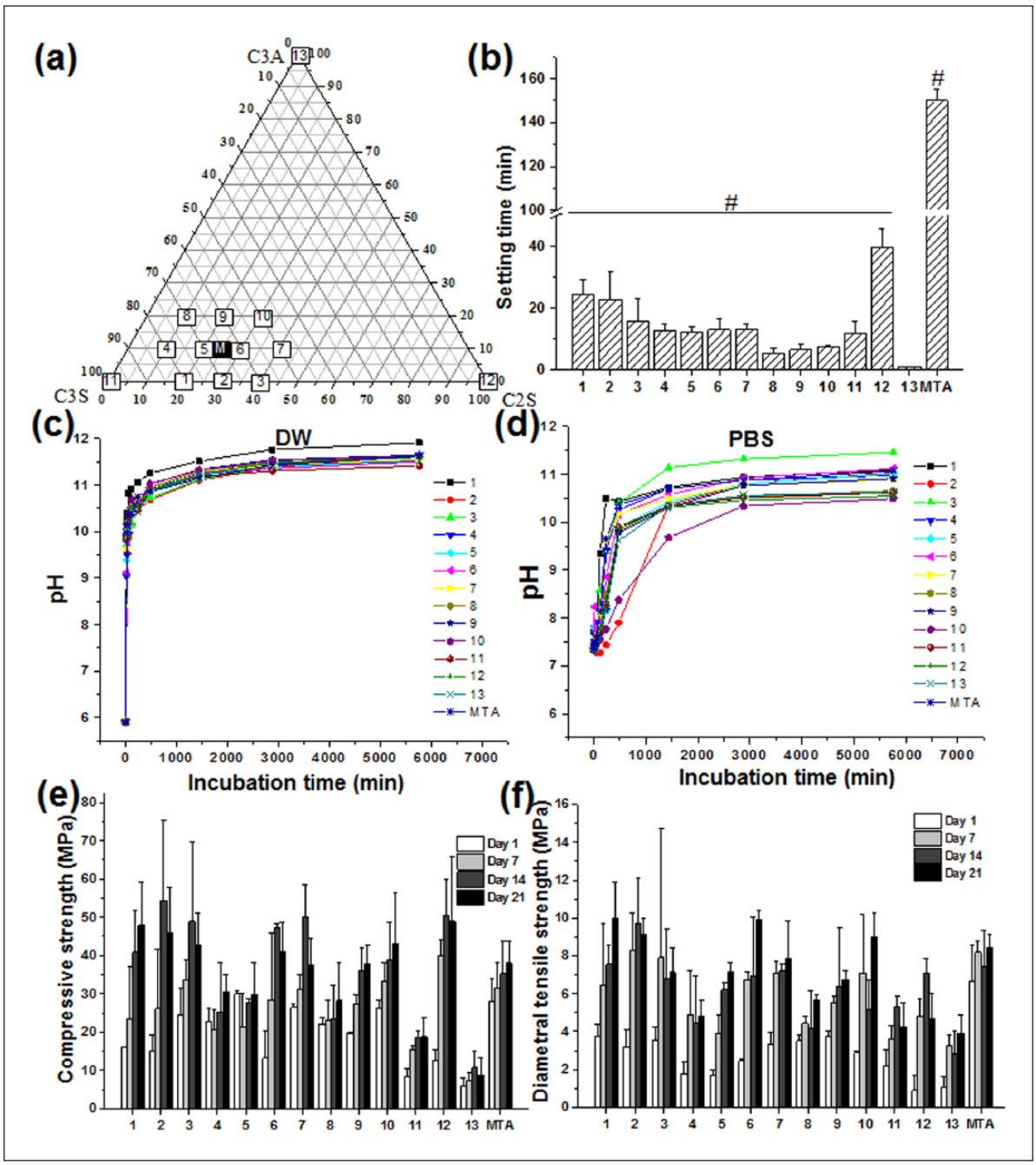

Figure 2. Physicomechanical properties of the cement. (a) Compositions of 14 types of cement were analyzed for (b) setting time (n = 5), (c) pH change (n = 3) in DW, (d) PBS, (e) compressive strength (n = 5), and (f) diametrical tensile strength (n = 5) in SBF are shown. C3A accelerated setting time while it had little effect on pH and changes in strength within 20% share in cement formula. Error bars representing standard deviation are plotted in each graph. Sharp (#) in setting time results indicate significant difference compared to group 13 (C3A) at <0.05. For the observation of trend of the effect of C3A, statistical analysis results omitted in other graphs.

and then a plateau at approximately pH 11–12 after 8 h (Figure 2(c)). The change in the pH of each sample measured in PBS was not as consistent as that of DW. Most specimens did not show much increase in pH and maintained a pH of approximately 7.5–8.5 until 2 h, except for group 1 (Figure 2(d)). After 2 days, all specimens exceeded a pH of 10 in PBS, except for group 10. On Day 4, all groups including MTA, C3S, C2S, and C3A showed pH values below 11, except for group 3 (C3S:C2S = 60:40). Other literature has reported pH of MTA or mixtures of the three compositions (C3S, C2S, and C3A) to range from 8 to 13 due to the release of hydroxyl ions during hydration

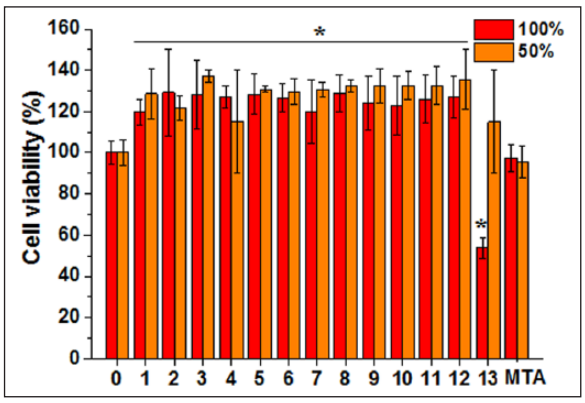

Figure 3. Cytocompatibility of the elute from the cement against rMSCs. The 100% extraction from C3A showed severe cytotoxicity compared to the control, while the others significantly increased cell viability (asterisk, $n = 4$, $p < 0.05$). Error bars representing standard deviation are plotted in each graph.

of the cement depending on the powder type, liquid mixed with the powder, and extraction solution.[31–33]

Mechanical properties of cements

The compressive strength and diametral tensile strength were measured after being incubated in SBF solution for up to 28 days (Figure 2(e) and (f)). Generally, the mechanical properties were enhanced with an increase in the incubation time in all groups, with a maximum strength of 2–4 times compared to that on Day 1 of incubation. Compressive and diametral tensile strength were found to be 8–49 MPa and 4–10 MPa, respectively, which were in the range of values reported in the previous literature regarding commercial MTA and calcium silicate cement.[27,31] The compressive strength of white MTA was reported to be 45.84 ± 1.32 MPa after 3 days,[31] and that of C3S cement was reported to be 17 MPa, which is similar to the value of 18.74 ± 4.9 MPa observed in this experiment.[27]

In vitro test showing cytotoxicity of C3A

In vitro cytocompatibility was performed with the extract of cement in culture media against rMSCs. After 24 h of co-culturing, a significant increase in cell viability (~120%) was observed in all groups except group 13 (C3A) compared to the media control, (Figure 3, $p < 0.05$) The aluminum containing C3A cement indicated the lowest cell viability (~60%, $p < 0.05$), while the other cements including even 20% C3A (G8, G9, and G10) did not exhibit cytotoxicity, and instead revealed increased cell viability. Aluminum ion is well-known to induce cytotoxicity against mammalian cells due to its destruction of lipid layer and DNA synthesis,[34,35] thus it is considered that the released aluminum ions from C3A (100% C3A) may be the major cause of C3A-induced cytotoxicity. In fact, other toxic metallic elements (e.g. Pb, Zn, Mg, Fe, and Bi) from the impurities in C3A, C3S, and C2S were trivial (less than 1 ppm), negating their possible cytotoxicity. When the fraction of C3A was below 20 wt% of cement (also for commercially available MTA formulation), the released aluminum ions may be below the threshold that exerts in vitro toxicity.[36] As to the C3A-induced cytotoxicity, Liu et al.[27] and Liu and Chang[28] reported that C3A/C3S or C3A/C2S complex containing 5, 10, or 15 wt% of C3A exhibited a level of toxicity to L929 cells, with the lowest cell viability observed for C3A (~60%, $p < 0.05$). Of note, a tendency of increased cytotoxicity with respect to C3A amount was noted. However, our study showed the C3A-induced cytotoxicity in a tertiary cement system—a composition more relevant to commercial MTA. Not only the toxicity issue but the therapeutic effects of the ternary reformulated cements on dental stem cells may warrant further study.[37,38]

Toxicity from C3A by intentional implantation of rat incisor

To scrutinize the biocompatibility of MTA, experimental cements with similar compositional combinations to conventional MTA and the single ingredient of MTA compositions (C2S, C3S, or C3A) were used for intentional implantation of teeth after root-end filling with cement. Cement groups with some representative compositions (G2, G5, G6, G9, C3S, C2S, C3A, and MTA) were chosen for the test (Figure 4(a)). A series of processes (tooth extraction, removal of pulp tissue in root canal, and retrofilling empty root canal with cement) were performed before re-implanting the tooth into the extracted site (Figure 4(b)). This in vivo model mimics the clinical application of MTA to the apical lesion of the tooth root, where MTA directly meets tissues for tissue regeneration.

According to the μCT picture in Figure 4(c), the G13 (C3A) group showed destruction of the hard tissue layer in the periapical area (white arrow), as well as alveolar bone below the apex of the tooth (dot rectangle), while the cement of the other groups and alveolar bone were separated by a radiopaque bone-like layer. A thin hard tissue layer at the interface of the cement and living tissue showed the bioactivity of the implanted materials.[29] In agreement with the previous literature, MTA showed great radiopacity (strong white color) with a conserved thin radiopaque layer at the interface between the cement at periapical lesion and surrounding alveolar bone. In many previous studies, MTA showed great biocompatibility compared to other materials such as amalgam and SuperEBA.[39,17] Especially in animal studies, the MTA generated newly formed bone, a pulp-dentin complex, or even cementum without an inflammatory reaction observed histologically.[40–42]

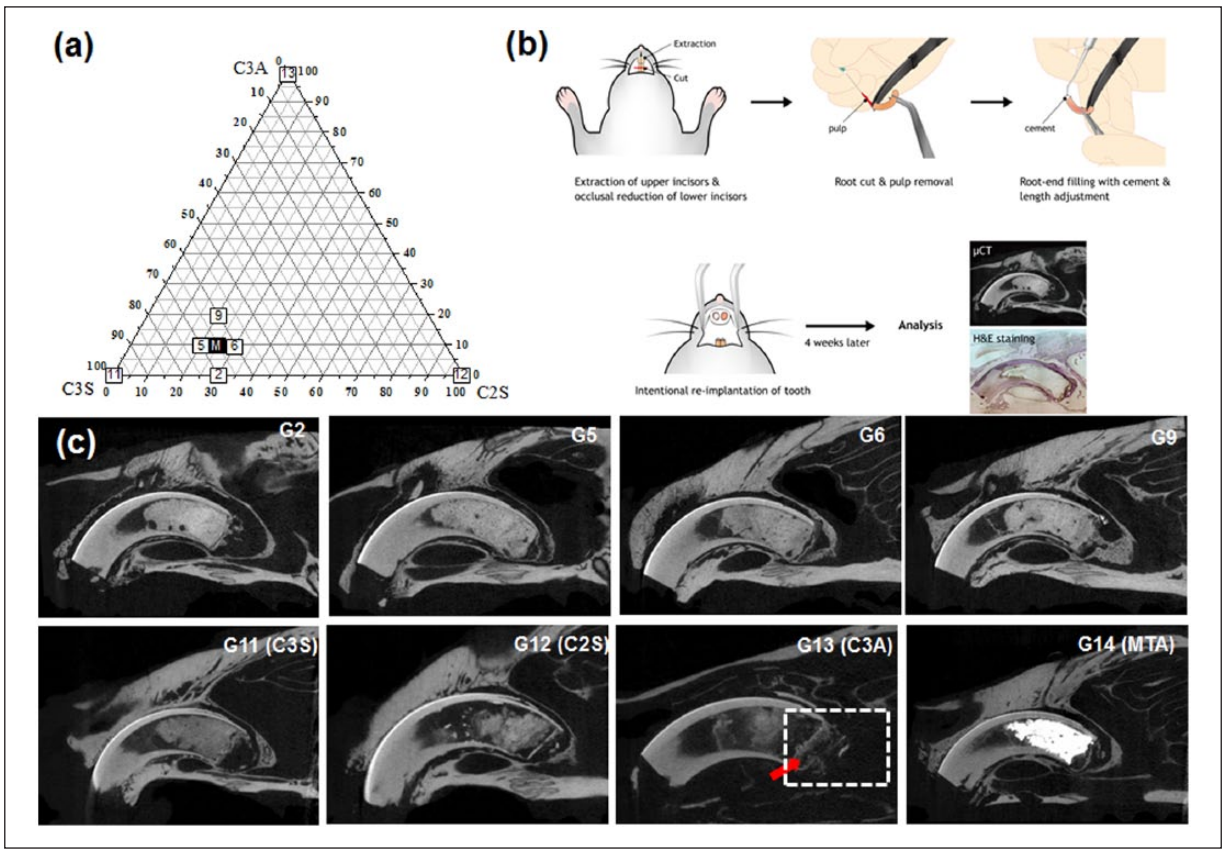

Figure 4. (a) Composition of the cements for the in vivo experiment. (b) Schematic image of the intentional implantation of the rat incisor after root-end filling with cement for investigation of the biocompatibility of the cement. (c) Images from the μCT after 4-week implantation. The red arrow in C3A indicates destruction of the thin radiopaque line at the material–tissue interface and the dashed rectangle shows alveolar bone surrounding the tooth, which was destroyed.

Therefore, to confirm the composition of the thin layer and inflammatory response, H&E staining was performed, and histological sections were visualized. In agreement with previous observations, MTA was located close to the alveolar bone without a significant inflammatory response (Figure 5, MTA). However, in G13 (C3A), a number of macrophages were shown to infiltrate into the periapical area which was still pronounced after 4 weeks of implantation. Due to the severity of inflammatory responses at the apex, the thin hard tissue layer separating the cement and the intact periapical lesion disappeared and the surrounding alveolar bone below the implanted cement was resorbed (Figure 5). In contrast, other groups revealed a well-developed thin osteo-dentin-like layer at the interface, separating the cement and the periapical alveolar bone lesion, which is a typical bioactive response of cements as reported elsewhere.[43,44]

Unlike experimental animal models such as dogs and monkeys, the incisor of the rat develops throughout its lifetime, and the cementum does not cover all the roots.[45] Therefore, the calcified substances, including thin hard tissue layer apically positioned, formed on the surface of all experimental specimens, were not from cementum; but the cementum-derived hard tissue formation will be the best scenario when MTA is applied to an apical lesion in clinical settings, thus studies with large animal models are needed in the future. Despite the limitations of the rat model and lack of the anatomical environment of humans (absence of cementum on the incisor and continuous tooth development) or evidence of the clinical performance of MTA, the biocompatibility and bioactivity of MTA compositions except C3A has been demonstrated in this study. Importantly, the possible adverse reaction from C3A in MTA indicates the need to develop aluminum-free MTA for safe and continuous use of MTA in humans, especially in children who are vulnerable to toxic events.

Conclusion

In this study, C3S, C2S, and C3A, which are major components of MTA, were successfully prepared with high purity to reveal the exact role of each component in the whole MTA cement system. The 10 components of C3S, C2S, and C3A with a close compositional ratio to MTA and 4 control groups (C3S, C2S, C3A, and MTA) were included in the analysis. All groups except MTA

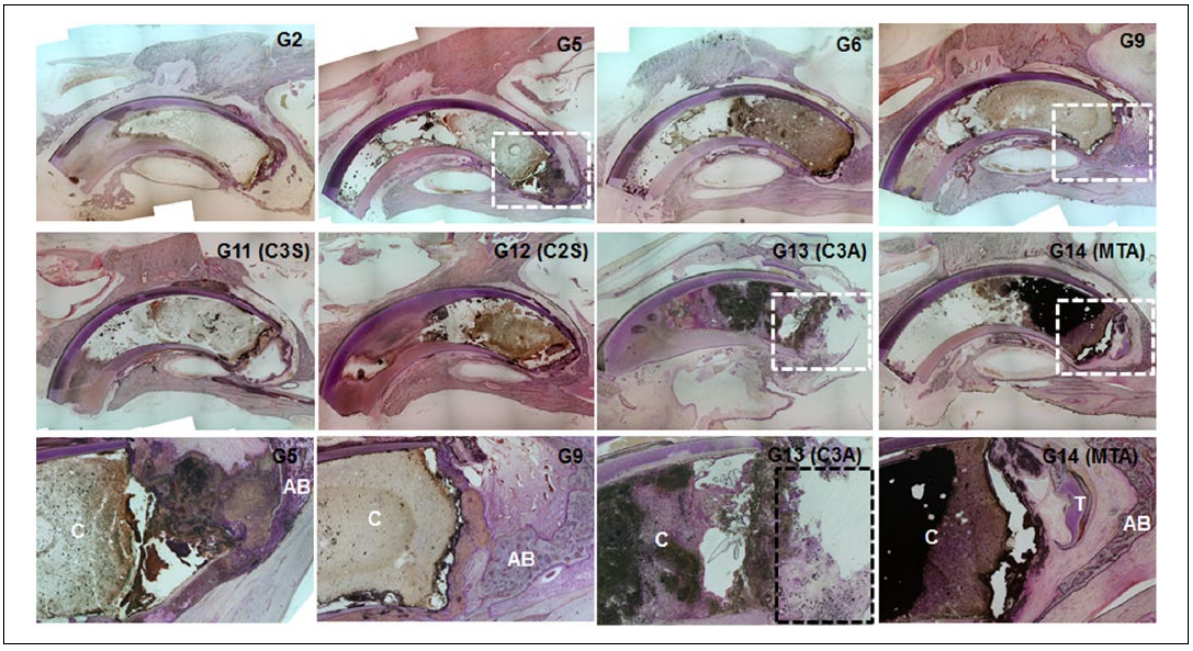

Figure 5. H&E staining images after 4 weeks of implantation are shown. The dashed rectangle indicates the site of magnification (C: cement, AB: alveolar bone, T: developing teeth). The dotted black line shows the destruction of alveolar bone surrounding tooth end. Severe inflammatory responses noted with a number of macrophages.

(~150 min) had setting times of less than 40 min, and the addition of C3A tended to accelerate the setting times. The pH abruptly increased initially and plateaued at 10–12 in both DW and PBS. Compressive and tensile strength also improved (2–4 times of initial values) with time for up to 21 days in SBF. The cytocompatibility tests with rMSC revealed cytotoxicity from the extraction of C3A, while the others showed increased cell viability. Intentional replantation of the rat incisor tooth after being filled with cement confirmed the adverse biological response of C3A at the tooth periapical region. Taken all of the three major constituents of the MTA, C3A has limited biocompatibility in vitro and in vivo although it can accelerate the initial hydration of cement. Therefore, a careful consideration of the compositional choice of MTA is necessary to minimize clinical failure due to compensated biocompatibility. This study suggests that, if possible (when other properties are satisfactory), the C3A component might be better avoided, which can be achieved by the mixture of the other individual components.

Acknowledgements

Ho-Jin Moon and Jung-Hwan Lee contributed equally to this paper as first authors.

Declaration of conflicting interests

The author(s) declared no potential conflicts of interest with respect to the research, authorship, and/or publication of this article.

Funding

The author(s) disclosed receipt of the following financial support for the research, authorship and/or publication of this article: This work was supported by the National Research Foundation of Korea (NRF) grant funded by the Korean Government (MSIP; Ministry of Science, ICT & Future Planning, NRF-2017R1C1B5076687, 2018R1D1A1B07042920, and 2018R1A2B3003446) and by Global Research Development Center Program (NRF-2018K1A4 A3A01064257).

References

1. Gandolfi MG, Siboni F and Prati C. Chemical–physical properties of pure dicalcium silicate, tricalcium silicate and MM-MTA. *Dent Mater* 2014; 30: e72–e73.
2. Bogen G and Kuttler S. Mineral trioxide aggregate obturation: a review and case series. *J Endod* 2009; 35(6): 777–790.
3. Taha NA, Ahmad MB and Ghanim A. Assessment of mineral trioxide aggregate pulpotomy in mature permanent teeth with carious exposures. *Int Endod J* 2017; 50(2): 117–125.
4. Dashnyam K, El-Fiqi A, Buitrago JO, et al. A mini review focused on the proangiogenic role of silicate ions released from silicon-containing biomaterials. *J Tissue Eng* 2017; 8: 1–13.
5. Islam MT, Felfel RM, Abou Neel EA, et al. Bioactive calcium phosphate-based glasses and ceramics and their biomedical applications: a review. *J Tissue Eng* 2017; 8: 1–16.
6. Ree MH and Schwartz RS. Long-term success of nonvital, immature permanent incisors treated with a mineral trioxide aggregate plug and adhesive restorations: a case series from a private endodontic practice. *J Endod* 2017; 43(8): 1370–1377.
7. Torabinejad M and Parirokh M. Mineral trioxide aggregate: a comprehensive literature review—part II: leakage

and biocompatibility investigations. *J Endod* 2010; 36(2): 190–202.
8. Camilleri J and Pitt Ford T. Mineral trioxide aggregate: a review of the constituents and biological properties of the material. *Int Endod J* 2006; 39(10): 747–754.
9. Parirokh M and Torabinejad M. Mineral trioxide aggregate: a comprehensive literature review—part I: chemical, physical, and antibacterial properties. *J Endod* 2010; 36(1): 16–27.
10. Camilleri J, Kralj P, Veber M, et al. Characterization and analyses of acid-extractable and leached trace elements in dental cements. *Int Endod J* 2012; 45(8): 737–743.
11. Fernández-Yáñez Sánchez A, Leco-Berrocal MI and Martínez-González JM. Metaanalysis of filler materials in periapical surgery. *Med Oral Patol Oral Cir Bucal* 2008; 13(3): E180–E185.
12. Torshabi M, Amid R, Kadkhodazadeh M, et al. Cytotoxicity of two available mineral trioxide aggregate cements and a new formulation on human gingival fibroblasts. *J Conserv Dent* 2016; 19(6): 522–526.
13. Ghatole K, Patil A, Giriyappa RH, et al. Evaluation of antibacterial efficacy of MTA with and without additives like silver zeolite and chlorhexidine. *J Clin Diagn Res* 2016; 10(6): ZC11–ZC14.
14. Kim SG, Malek M, Sigurdsson A, et al. Regenerative endodontics: a comprehensive review. *Int Endod J*. Epub ahead of print 19 May 2018. DOI: 10.1111/iej.
15. Tsesis I, Elbahary S, Venezia NB, et al. Bacterial colonization in the apical part of extracted human teeth following root-end resection and filling: a confocal laser scanning microscopy study. *Clin Oral Investig* 2018; 22(1): 267–274.
16. Chang S-W, Baek S-H, Yang H-C, et al. Heavy metal analysis of ortho MTA and ProRoot MTA. *J Endod* 2011; 37(12): 1673–1676.
17. Tanomaru-Filho M, Andrade A, Rodrigues EM, et al. Biocompatibility and mineralized nodule formation of Neo MTA Plus and an experimental tricalcium silicate cement containing tantalum oxide. *Int Endod J* 2017; 50: e31–e39.
18. ISO 6876. *Root canal sealing materials*. Geneva: International Standardization Organization, 2012.
19. Kim D-A, Lee J-H, Jun S-K, et al. Sol-gel-derived bioactive glass nanoparticle-incorporated glass ionomer cement with or without chitosan for enhanced mechanical and biomineralization properties. *Dent Mater* 2017; 33(7): 805–817.
20. Kim TH, Kim M, Eltohamy M, et al. Efficacy of mesoporous silica nanoparticles in delivering BMP-2 plasmid DNA for in vitro osteogenic stimulation of mesenchymal stem cells. *J Biomed Mater Res A* 2013; 101A(6): 1651–1660.
21. Nishioka M, Shiiya T, Ueno K, et al. Tooth replantation in germ-free and conventional rats. *Endod Dent Traumatol* 1998; 14(4): 163–173.
22. Katsamakis S, Slot DE, Van der Sluis LW, et al. Histological responses of the periodontium to MTA: a systematic review. *J Clin Periodontol* 2013; 40(4): 334–344.
23. Lee J-H, Mandakhbayar N, El-Fiqi A, et al. Intracellular co-delivery of Sr ion and phenamil drug through mesoporous bioglass nanocarriers synergizes BMP signaling and tissue mineralization. *Acta Biomater* 2017; 60: 93–108.
24. Lee JH, El-Fiqi A, Mandakhbayar N, et al. Drug/ion co-delivery multi-functional nanocarrier to regenerate infected tissue defect. *Biomaterials* 2017; 142: 62–76.
25. Camilleri J, Montesin FE, Brady K, et al. The constitution of mineral trioxide aggregate. *Dent Mater* 2005; 21(4): 297–303.
26. Torabinejad M, Hong C, McDonald F, et al. Physical and chemical properties of a new root-end filling material. *J Endod* 1995; 21(7): 349–353.
27. Liu WN, Chang J, Zhu YQ, et al. Effect of tricalcium aluminate on the properties of tricalcium silicate-tricalcium aluminate mixtures: setting time, mechanical strength and biocompatibility. *Int Endod J* 2011; 44(1): 41–50.
28. Liu W and Chang J. Setting properties and biocompatibility of dicalcium silicate with varying additions of tricalcium aluminate. *J Biomater Appl* 2012; 27(2): 171–178.
29. Kang MS, Lee N-H, Singh RK, et al. Nanocements produced from mesoporous bioactive glass nanoparticles. *Biomaterials* 2018; 162: 183–199.
30. Rodger SA and Double DD. The chemistry of hydration of high alumina cement in the presence of accelerating and retarding admixtures. *Cement Concrete Res* 1984; 14(1): 73–82.
31. Islam I, Chng HK and Yap AUJ. Comparison of the physical and mechanical properties of MTA and Portland cement. *J Endod* 2006; 32(3): 193–197.
32. Massi S, Tanomaru-Filho M, Silva GF, et al. pH, calcium ion release, and setting time of an experimental mineral trioxide aggregate-based root canal sealer. *J Endod* 2011; 37(6): 844–846.
33. Ding SJ, Kao CT, Shie MY, et al. The physical and cytological properties of white MTA mixed with Na2HPO4 as an accelerant. *J Endod* 2008; 34(6): 748–751.
34. Domínguez C, Moreno A and Llovera M. Aluminum ions induce DNA synthesis but not cell proliferation in human fibroblasts in vitro. *Biol Trace Elem Res* 2002; 86(1): 1–10.
35. Kanjevac TV, Milovanović MZ, Milošević-Djordjević O, et al. Cytotoxicity of glass ionomer cement on human exfoliated deciduous teeth stem cells correlates with released fluoride, strontium and aluminum ion concentrations. *Arch Biol Sci* 2015; 67(2): 619–630.
36. Gandolfi MG, Siboni F, Primus CM, et al. Ion release, porosity, solubility, and bioactivity of MTA Plus tricalcium silicate. *J Endod* 2014; 40(10): 1632–1637.
37. Chalisserry EP, Nam SY, Park SH, et al. Therapeutic potential of dental stem cells. *J Tissue Eng* 2017; 8: 1–17.
38. Sharmin N, Gu F, Ahmed I, et al. Compositional dependency on dissolution rate and cytocompatibility of phosphate-based glasses: effect of B2O3 and Fe2O3 addition. *J Tissue Eng* 2017; 8: 1–10.
39. Torabinejad M, Watson T and Pitt Ford TR. Sealing ability of a mineral trioxide aggregate when used as a root end filling material. *J Endod* 1993; 19(12): 591–595.
40. Baek S-H, Lee WC, Setzer FC, et al. Periapical bone regeneration after endodontic microsurgery with three different root-end filling materials: amalgam, SuperEBA, and mineral trioxide aggregate. *J Endod* 2010; 36(8): 1323–1325.
41. Baek S-H, Plenk H and Kim S. Periapical tissue responses and cementum regeneration with amalgam, superEBA, and MTA as root-end filling materials. *J Endod* 2005; 31(6): 444–449.
42. Hsu TT, Yeh CH, Kao CT, et al. Antibacterial and odontogenesis efficacy of mineral trioxide aggregate combined with CO2 laser treatment. *J Endod* 2015; 41(7): 1073–1080.

43. Bernabé PF, Holland R, Morandi R, et al. Comparative study of MTA and other materials in retrofilling of pulpless dogs' teeth. *Braz Dent J* 2005; 16(2): 149–155.
44. Torabinejad M, PittFord TR, McKendry DJ, et al. Histologic assessment of mineral trioxide aggregate as a root-end filling in monkeys. *J Endod* 1997; 23(4): 225–228.
45. Stern IB. An electron microscopic study of the cementum, Sharpey's fibers and periodontal ligament in the rat incisor. *Am J Anat* 1964; 115(3): 377–409.